DNA methylation regulates glioma cell cycle through down-regulating MiR-133a expression

Liang Liu
Second Affiliated Hospital of Shenzhen University
Zhengquan Zhu
The 3rd Affiliated Teaching Hospital of Xinjiang Medical University
Xu Li
Second Affiliated Hospital of Shenzhen University
Yong Zheng (yongzsz7@163.com)
Second Affiliated Hospital of Shenzhen University https://orcid.org/0000-0002-8676-5279

Research article

Keywords: Glioma; DNA methylation; miR-133a; PPARγ

Posted Date: February 7th, 2020

DOI: https://doi.org/10.21203/rs.2.17676/v2

Abstract

Background: MiRNAs plays a key role in regulating gene expression networks of various biological processes in many cancers. Results: Here, we analyzed miRNA expression profiles by miRNA microarray and verified by RT-PCR. It was shown that the expression difference of miR-133a was most significantly and consistently downregulated. The proliferative capacity and cell cycle profile of cells transfected with miR-133a mimic were assessed by colony forming assay and PI staining, respectively. The target gene of miR-133a was predicted using TargetScan and verified by dual luciferase gene reporter assay. Western blotting and RT-PCR were used to analyze the expression levels of relevant factors. Methylation-specific quantitative PCR (MSP) was used to detect miR-133a methylation levels. Epigenetic regulation of miR-133a was assessed by treating the cells with the DNA methyltransferase inhibitor AZA or the histone deacetylase inhibitor TSA. We found that overexpression of miR-133a inhibited cell proliferation, induced a cell cycle arrest and downregulated the expression of Cyclin D1, Cyclin D2, and cycling-dependent killdeer 4 (CdK4). Peroxisome proliferator-activated receptor γ (PPARγ) was verified as a target gene of miR-133a. PPARγ protein levels were significantly higher in the glioma tissues, and overexpression of miR-133a markedly reduced its levels. Furthermore, forced expression of PPARγ partly abrogated the anti-proliferative effects of miR-133a. miR-133a was hypermethylated in glioma cells, and AZA treatment significantly up-regulated its levels. Conclusions: MiR-133a is downregulated in glioma cells through promoter hypermethylation, and its forced expression inhibits glioma cell proliferation and induces G1 phase arrest by targeting PPARγ.

Background

Gliomas are the most common primary tumors of the central nervous system, and account for about 40%-60% of all intracranial tumors[1]. Although the diagnosis and treatment of glioma have improved in recent years, the clinical outcome is still very poor. The five-year survival rate of patients with medium to low-grade glioma is 30%-70%, while those with high-grade gliomas have a dismal median survival duration of 14 months and a five-year survival rate of less than 3%[2]. Therefore, it is essential to identify the molecular mechanisms underlying glioma initiation and development in order to reduce the incidence and mortality of glioma, and improve patient prognosis.

MicroRNAs (miRNAs) are a class of endogenous single-stranded non-coding small RNAs that can bind to the 3' untranslated region (UTR) of a target mRNA through complementary base pairing, and either degrade or inhibit the translation of the transcript[3]. Recent studies have established a key role of miRNAs in regulating the gene expression networks in cell cycle progression, proliferation, differentiation and apoptosis, as well as inflammation, stress responses and various pathological conditions. In addition, analyses of the aberrant expression profiles of miRNAs in specific diseases have helped identify the miRNAs associated with these diseases. For instance, associated aberrant expression levels of miR-191 and miR-193a in melanoma patients with reduced survival[4]. Similarly, the downregulation of miR-1247 in osteosarcoma inhibits tumor progression through MAP3K9 regulation[5]. In glioma tissues and cells, multiple miRNAs like miR-21[6], miR-128-3p[7], miR-92b[8] and miR-125b[9] are abnormally

expressed, and associated with tumorigenesis and progression. Studies show that epigenetic mechanisms, such as DNA methylation, play an important role in regulating miRNA expression[10, 11]. In fact, the hypermethylation of the CpG islands in the promoter regions of tumor-suppressing miRNAs is one of the most common mechanisms of their downregulation during tumorigenesis[12].

PPARγ is a peroxisome proliferator-activated receptor that belongs to type II nuclear hormone receptor family, and elicits numerous biological effects upon ligand binding and activation[13]. Recent studies show that activated PPARγ in tumor cells leads to the constitutive activation of various signaling pathways[14]. In pancreatic cancer cells for example, activated PPARγ can induce differentiation, regulate cell cycle and modulate the expression levels of apoptotic and anti-apoptotic genes, thus driving tumor growth[15]. Furthermore, rosiglitazone-mediated activation of PPARγ in the liver cancer cell line SMMC7221 led to cell cycle arrest at the G1 phase, and also affected the levels of γ-glutamyltransferase and alpha-fetoprotein, which are differentiated from hepatoma cells[16]. MiR-133a is a member of the miR-133 family. Recent studies showed that the miR-133a expression level in glioma tissue is remarkable low[17], and further studies suggested that miR-133a involved in regulating the proliferation and apoptosis of glioma cells. Substantial evidence shows that miR-133a acts as a cancer suppressor, and lower expression of miR-133a in cancer patients is associated with poor prognosis[18,26]. In this study, we compared the miRNA expression profiles of glioma and normal brain tissues, and found that the expression level of miR-133a was significantly lower in glioma tissues, and further discussed through RT-PCR, MTT, bioinformatics and other related experiments in order to explore the related regulatory mechanisms to obtain novel insights for treating glioma and improving its prognosis.

Results

MiR-133a is downregulated in glioma cells

The hierarchical clustering analysis were used to reveal distinctive miRNA expression patterns between cancerous tissue and normal tissue, and we found that the miRNA microarrays of glioma and normal brain tissues revealed 81 differentially-expressed miRNAs, of which 28 were up-regulated and the remaining were down-regulated. In addition, 15 miRNAs were consistently up- or down-regulated in all three glioma tissue samples (Fig 1A), of which miR-133a showed the most significant down-regulation (Supplementary Table-2). Our gene chip data posted on http://www.xjmu.edu.cn/. Subsequent RT-PCR validation on all tissue samples confirmed that miR-133a levels were significantly lower in the gliomas compared to normal brain tissues (Fig. 1B; $p<0.01$). Consistent with this, miR-133a was significantly downregulated in the glioma cell lines U251, U87, T98-G and A172 compared to that in the normal glial cell line HEB (Fig. 1C; $p<0.01$). Furthermore, the incidence of low levels of miR-133a in glioma patients was also evaluated with the TCGA dataset, and consistent with the above results, the expression of miR-133a was significantly higher in glioma patients than in non-tumor brain tissue (Fig. 1D; $p<0.01$). Next, in virtue of the TCGA dataset, association between miR-133a expression and overall survival were investigated in glioma patients using the Kaplan-Meier survival analysis. The results showed that low expression levels of miR-133a were significantly correlated with short overall survival (OS) in comparison

to high miR-133a levels (Fig. 1E; $p<0.05$). These data suggested that miR-133a could be a prognosis biomarker for glioma patients and miR-133a might participate in glioma genesis.

Overexpression of miR-133a inhibits the proliferation of glioma cells

The miR-133a^{hi} A172 cells and miR-133a^{lo} U251 cells were each transfected with the miR-133a mimic, which significantly increased the expression of miR-133a compared to that in the un-transfected controls ($p<0.01$). However, miR-NC had no effect on miR-133a expression levels ($p>0.05$), indicating the specificity of the miRNA constructs (Fig. 2A). Mir-133a overexpression significantly decreased the proliferative capacity of both the A127 and U251 cells compared to the respective controls (Fig. 2B; $p<0.01$). Consistent with this, the colony formation ability of the cells transfected with miR-133a also decreased significantly compared to the controls (Fig. 2C; $p<0.01$). Taken together, miR-133a inhibits the proliferation of glioma cells.

MiR-133a targets PPARγ in glial glioma cells

The TargetScan database screening predicted a complementary sequence for miR-133a in the 3'-UTR of PPARγ gene, suggesting that the latter is a target gene of miR-133a (Fig. 3A). Dual luciferase gene reporter assay further showed a significant decrease in luciferase activity in cells co-transfected with the miR-133a mimic and PPARγ WT plasmids. However, co-transfection with miR-133a mimic and PPARγ mutant (MUT) plasmids, or miR-133a NC and PPARγ WT/MUT plasmids did not result in any obvious changes in luciferase activity (Fig. 3B). These results indicated that PPARγ is a target gene of miR-133a, and is likely suppressed by the latter. Furthermore, PPARγ protein expression was significantly increased in both glioma tissues and miR-133a-overexpressing cell lines compared to the respective controls (Fig. 3C; $p<0.01$ for both), which confirmed its downregulation by miR-133a.

MiR-133a inhibits proliferation of glioma cells by targeting PPARγ

Given that miR-133a direct targeted the 3’-UTR of PPARγ and repressed its expression, we asked whether downregulation of PPARγ was the mechanistic basis of the inhibitory effect of miR-133a on glioma cells. We co-transfected PPARγ and miR-133a mimic into A172 cells and then investigated the cell proliferation activity. The MTT assay results showed that cells co-transfected miR-133a mimic and pcDNA3.1-PPARγ (PPARγ) enhanced glioma cell viability compared to cells transfected with the miR-133a mimic and empty vector (vector) (Fig. 4A). In addition, increased colony forming ability was also observed in cells co-transfected with miR-133a mimic and PPARγ compared to those co-transfected with the miR-133a mimic and vector (Fig. 4B). Taken together, miR-133a exerts its inhibitory effects in glioma cells by suppressing PPARγ expression, and restoring the latter can abrogate miR-133a-mediated inhibition.

MiR-133a overexpression induces cell cycle arrest in glioma cells

Overexpression of miR-133a significantly increased the proportion of glioma cells in the G1 phase compared to that in the controls (Fig. 5A; $p<0.05$). Furthermore, the A172 and U251 overexpressing miR-

133a showed a significant decrease in the expression levels of proteins driving G1 to S phase transition, including Cyclin D1, Cyclin D2 and CDK4, compared to the cells transfected with miR-NC (Fig. 5B; $p<0.05$). Taken together, miR-133a inhibits the proliferation of glioma cells by arresting the cell cycle at the G1 phase.

Effect of DNA methylation on the expression of miR-133a in glioma cells

We searched for putative CpG islands upstream of miR-133a gene (-1200) using the prediction website http://cpgislands.usc.edu, and detected one CpG island in the promoter region (Fig. 6A). To determine whether DNA methylation affected the expression of miR-133a in glioma cells, we analyzed its levels after treating the cells with the methylation inhibitor AZA or the acetylase inhibitor TSA. While AZA significantly upregulated miR-133a in the glioma cells lines ($p<0.01$), TSA had no significant effect, indicating that DNA methylation rather than acetylation is the epigenetic mechanism regulating miR-133a (Fig. 6B). Furthermore, MSP showed significantly greater methylation in the miR-133a CpG islands in the glioma cell lines compared to the normal glial cells ($p<0.01$), which was decreased to normal levels in the presence of AZA (Fig. 6C). Taken together, hypermethylation of the miR-133a promoter in glioma cells significantly downregulates its levels, and reducing methylation at this site can restore miR-133a expression.

Discussion

Glioma is the most common primary malignant tumor of the central nervous system. Due to its highly invasive nature, high mortality rate and poor therapeutics[19], it is essential to unravel the genes and signaling pathways driving glioma development, in order to devise novel strategies for its diagnosis and treatment.

MiRNAs are non-coding RNAs about 20-25 nucleotides in length. Since its discovery by Lee et al. in nematodes in 1993, over 2,000 mature miRNAs have been identified in humans that regulate the expression of approximately 30% of the total genes. MiRNAs regulate multiple functions, including cell proliferation, cell cycle, apoptosis and differentiation[20-24]. MiR-133a is downregulated in various cancers and acts as a tumor suppressor. It is expressed at low levels in renal cancer tissues and cell lines, and its forced expression inhibited the proliferation and invasion of renal cancer cells, induced apoptosis and arrested cell cycle progression by targeting TAGLN2[25]. Similarly, Cheng et al. found that miR-133 was downregulated in gastric cancer tissues, and inhibited the proliferation, invasion and metastasis of gastric cancer cells by targeting the CDC42/PAKs signaling pathway[26]. Furthermore, low expression levels of miR-133a was significantly correlated with poor prognosis of gastric cancer patients. In a recent study, miR-133a was also significantly decreased in glioma tissues, and might through suppressing the expression level of epidermal growth factor receptor (EGFR) to inhibit the glioma cell proliferation and apoptosis. However, the molecular mechanism of downregulation of miR-133a expression had not been further investigated[17].

In this study, we screened the miRNA expression profiles of glioma and normal brain tissues, and detected consistent and significant downregulation of miR-133a in the former, which was also confirmed by RT-PCR. In addition, miR-133a expression was also significantly decreased in glioma cell lines compared to that in a normal glial cell line. By mining the miRNA-Seq data of glioma in TCGA dataset, we found that miR-133a was also significantly lower expressed in large samples of glioma tissues, and survival analysis confirmed that the overall survival time of glioma patients with low expression of miR-133a was significantly lower than that of patients with high miR-133a expression. These results suggest that miR-133a plays a role of tumor suppressor genes in the occurrence and development of glioma, and its low expression may lead to poor prognosis in glioma patients. To further investigate the relationship between miR-133a and glioma, the following studies were performed. Forced expression of miR-133a in the glioma cells significantly inhibited their proliferative and colony forming abilities, indicating that it acts as a tumor suppressor in glioma. Furthermore, *in silico* target prediction identified PPARγ as a target gene of miR-133a, which was verified by dual luciferase gene reporter assay. Consistent with this, PPARγ protein levels were significantly higher in glioma tissues compared to normal brain tissues, and decreased in glioma cells following miR-133a overexpression. Thus, miR-133a likely binds to the 3'UTR of PPARγ and inhibits its expression.

Forced expression of PPARγ in the miR-133a-overexpressing cells rescued them from the inhibitory effects of the latter, which further indicated that the targeted suppression of PPARγ by miR-133a is the mechanistic basis of its action. Studies show that PPARγ activation upregulate Cyclin Ds, Cyclin E and CDK4, which accelerates cell cycle progression and cell proliferation[27-29]. Cyclin D1 is a key regulatory protein of the mammalian cell cycle which binds to the downstream Cyclin D2 and cyclin-dependent kinase CDK4 to form a complex that phosphorylates the retinoblastoma protein (Rb). This releases the nuclear transcription factor E2F from Rb, and promotes its nuclear translocation to transcriptionally activate genes involved in G1 to S phase transition, finally enabling the cells to enter a proliferative state [30]. Overexpression of miR-133a in glioma cells induced cell cycle arrest at the G1 phase, and downregulated Cyclin D1, Cyclin D2 and CDK4 proteins.

Studies show that epigenetic mechanisms like DNA methylation and histone acetylation play key roles in regulating miRNA expression [12]. Since aberrant epigenetic regulation of tumor-suppressors is often observed in cancer[31-34], we next analyzed the levels of miR-133a in glioma cells after specifically inhibiting DNA methyltransferase or histone deacetylase. MiR-133a was significantly upregulated by AZA but not by TSA, indicating that DNA methylation and not histone deacetylation regulates miR-133a levels in glioma cells. Furthermore, MSP assay showed that the methylation level of miR-133a was significantly higher in glioma cells compared to that in normal glial cells. This suggested that the CpG islands in the miR-133a gene promoter region are hypermethylated in glioma cells, which leads to its downregulation. Therefore, reducing methylation at this site can restore miR-133a expression in glioma cells, and can be explored as a therapeutic strategy.

Conclusions

MiR-133a is downregulated in glioma tissues through promoter hypermethylation, and its forced expression inhibits glioma cell proliferation and induces G1 phase arrest by targeting PPARγ. However, further research is needed to determine other functions of miR-133a in glioma and elucidate the underlying mechanisms.

Methods

Tissue samples

This study was approved by the Ethics Committee of Second Affiliated Hospital of Shenzhen University (SSZU20180307). All samples and data were collected after obtaining the statement on informed consent from the glioma patients or the legally authorized representatives of healthy controls with brain trauma. Fifteen surgically excised glioma tissue samples were collected at our hospital from August 2018 to August 2019, and glioma was confirmed by clinical and pathological examination. Eight of the 15 samples were obtained from male patients and 7 from female patients, with an average age of 52.3 ± 6.9 years. The histological diagnosis of glioma was based on the Central Nervous System Tumor Grading Criteria[31] established by WHO in 2016. Three cases were grade I tumors, 5 grade II, 3 grade III and 4 grade IV（Supplementary Table-1）. Furthermore, brain tissues were removed from 15 age-matched healthy controls with brain trauma (9 males and 6 females, average age 52.8 ± 7.4 years) during intracranial decompression. The differences of the two groups' gender, age have no statistical significance(P>0.05), and the materials have good comparability. The inclusion criteria for the patients were: 1) primary tumor occurrence, and 2) lack of radiotherapy, chemotherapy or any treatment before surgery. The tissue specimens were flash frozen in liquid nitrogen, and stored at -80°C.

Cell lines and main reagents

The human normal glial cell line HEB and glioma cell lines U251, U87, T98-G and A172 were purchased from the Cell Resource Center of Shanghai Institutes for Biological Sciences, Chinese Academy of Sciences. DMEM/HG, fetal bovine serum (FBS), Opti-MEM and 0.25% trypsin containing 0.02% EDTA were purchased from Gibco, MTT kit, 5-aza-2'-deoxycytosine (AZA) and histone deacetylase inhibitor (TSA) from Sigma, Trizol, reverse transcription kit from Thermo, SYBR Green Real-time PCR kit from Shanghai Solarbio Bioscience & Technology, QIAamp DNA Mini kit and EpiTect Bisulfite kit from Qiagen, Lipofectamine 3000 from Invitrogen, and the cell cycle assay kit from BD. The pcDNA3.1-miR-133a mimic, scrambled miRNA (miR-NC) and the pcDNA3.1-PPARγ overexpression plasmid were obtained from Guangzhou Ruibo Bio. Antibodies against PPARγ, cyclin D1, cyclin D2, CDK4 and β-actin were from Abcam, and the horseradish peroxidase (HRP)-labeled IgG secondary antibody from Guangzhou Jingcai. PPARγ wild type (WT) and mutant (MUT) luciferase reporter plasmids were purchased from Shanghai Jima and the luciferase assay kit from Promega. The PCR primers were synthesized by Shanghai Shenggong. Other reagents were from our laboratory and of analytical grade.

Cell culture and transfection

The cell lines were thawed, and cultured at 37°C under 5% CO_2 in DMEM/HG containing 10% FBS. The cells were harvested by trypsin digestion once they were 70%-80% confluent, centrifuged at 800 rpm for 5 min at room temperature, and resuspended in DMEM/HG for further passaging. Cell transfection was performed as previously described[7, 9]. Briefly, for the transfection of A172 and U251 cells, they were harvested at 80% confluency, re-suspended in Opti-MEM, and seeded in a 6-well plate at the density of 2×10^5 per well. Following overnight incubation, the cells were transfected with 100 ng pcDNA3.1-PPARγ or 50nM pcDNA3.1-miR-133a mimic and pcDNA3.1-miR-NC (using Lipofectamine 3000 according to the manufacturer's instructions. Six hours later, the medium was replaced with DMEM/HG containing 10% FBS, and the cells were cultured for another 48h. The medium was replaced with complete DMEM/HG containing 2μg/ml puromycin, and the cells were cultured for 3 days. The transfected cells were re-plated and after 1-2 weeks, the resulting clones were expanded to establish stable miR-133a mimic and miR-NC cell lines.

miRNA microarray analysis

Three tissue samples each from glioma patients and healthy controls were sent to Shanghai Kangcheng Biotechnology Co. Ltd. for miRNA microarray analysis. Briefly, total RNA was extracted from the tissues using Trizol reagent, and purified with a miRNA Mini kit according to the instructions. The purity and concentration of the RNA samples were analyzed using a spectrophotometer, and 1μg RNA per sample was labeled using a Hy3/Hy5 Power Labeling kit according to the instructions. The labeled RNA was then hybridized with a miRCURY^{tm} LNA Array, and the original signal intensity of the chip was tested using a GenePix 4000B chip scanner. Using intensity (int) > 50 as the normalization factor, the differences in miRNA expression levels between the glioma and normal tissue samples were analyzed by inter-chip standardization, intra-chip standardization, expression difference comparison, statistical significance test, and cluster analysis. In this experiment, the seventh generation of miRCURYTMLNA hybrid chip(v.18.0) (Exiqon) was used to test the samples, containing 3100 species of probe. For the specific probe ID, please refer to http://www.kangchen.com.cn/support/supportmain.asp? Id = 21.

TCGA dataset with patient information

R2.15.3 Epicalc fuction package was used to download and preprocess the expression of miR-133a miRNA SeqV2 data and the corresponding pathological data of the glioma data set from TCGA database (https://tcga-data.nci.nih.gov/tcga/). Expression of miR-133a and survival analysis of glioma patients were as previously described[7, 9]. Briefly, the level 3 data of qualified miR-133a expression with clinical information of glioma patients were obtained from TCGA data portal. We obtained 725 samples, which included 518 glioma samples and 207 non-tumor brain samples. And there were qualified clinical information of 479 glioma patients corresponding to miR-133a expression in samples. To avoid the impact of unrelated causes of death, the cases with less than 1-month overall survival and death from other diseases or accidents were excluded in this study. As a result, 463 patients fitted this criterion for overall survival analysis. The 50% of the sorted miR-133a values was set as cut-off for low/high expression of miR-133a.

Cell proliferation assay

The miR-133a mimic and miR-NC-transfected cells were seeded into 96-well plates at the density of 2×10^4 per well in 200μl complete DMEM/HG medium. After culturing for 12, 24, 36 and 48h, 20μl MTT reagent (5mg/ml) was added to each well, and the cells were incubated further for 4h. The culture medium was removed, and 150μl dimethyl sulfoxide (DMSO) was added per well to solubilize the formazan crystals. After shaking for 10 min at room temperature, the absorbance value (OD_{490}) of each well was measured at 490 nm. Each time point per group was tested in five replicate wells, and the mean values were calculated.

Colony formation assay

A colony formation assay was performed as previously described[16]. Briefly the miR-133a and miR-NC-transfected cells were seeded into 6-well plates at the density of 1×10^3 cells/well. The cells were cultured for 8 days, and the medium was changed every 3 days. The resulting colonies were fixed with 3.7% paraformaldehyde for 5 min, stained with 0.05% crystal violet for 20 min at room temperature, and gently washed with double distilled water five times. The number of colonies were counted under a white light microscope.

Western blotting

Protein levels were determined by Western blots as previously described [7-9]. Briefly, the suitably transfected cells were washed thrice with cold PBS at 4°C, lysed with RIPA cell lysis buffer supplemented with a protease inhibitor, and centrifuged at 4°C and 12,000 rpm for 20 min. The supernatants were aspirated and the protein concentration was determined by the BCA method. Equal amounts of protein per sample (30μg) were mixed with 5× loading buffer at the ratio of 4:1, and denatured by boiling for 10 min. The protein samples were resolved by SDS-PAGE, and the bands were transferred to PVDF membranes by the wet transfer method. The membranes were blocked with 5% skim milk at room temperature for 2h, and incubated overnight with primary antibodies against PPARγ (1:500), cyclin D1 (1:500), cyclin D2 (1:500) or CDK4 (1:500), and β-actin (1:1000) at 4°C on a shaker. After washing thrice with TBST buffer, the membranes were incubated with a horseradish-labeled secondary antibody (1:2,000) for 1h at room temperature, followed by three more washes with TBST. The blots were then developed using an ECL solution and photographed on a gel imager. The Image J software was used to measure the gray value of each band, and the ratio of the intensities of the target proteins to that of the internal control β-actin was calculated. The experiment was repeated thrice.

Dual luciferase gene reporter assay

The online database TargetScan was screened for the putative target genes of miR-133a. To validate PPARγ as a target, the dual luciferase reporter assay was performed. The dual luciferase gen reporter assay was previously described [20,22]. Briefly, A172 and U251 cells were harvested in the logarithmic growth phase and seeded in 96-well plates at the density of 2×10^4 cells/well. Following overnight culture,

the cells were co-transfected with luciferase reporter plasmids harboring wild type (WT) or mutated PPARγ promoter sequences, and miR-133a mimic or miR-NC using Lipofectamine 3000. Each group was tested in five replicates. After 48 hours, the fluorescence intensity of firefly luciferin and Renilla fluorescein was detected according to the instructions of dual luciferase assay kit.

Propidium iodide staining

Propidium iodide staining was performed as previously [15]. Briefly, the suitably transfected A172 and U251 cells were gently washed with cold PBS, harvested, and centrifuged at 300 rpm for 5 min at room temperature. The supernatant was removed, and the cells were re-suspended in 500μl PBS. Ice-cold 70% alcohol (3.5 ml) was added immediately, and the cells were thoroughly pipetted and fixed overnight at 4°C. After washing thrice with PBS, the cells were stained with 500μl PI/RNase staining solution provided in the cell cycle flow detection kit for 30 min at 4°C in the dark. The cell cycle distribution was analyzed by flow cytometry. The experiment was repeated thrice.

Drug treatment

HEB, A172 and U251 cells were harvested and seeded in a 6-well plate at the density of 1×10^5/well, and cultured till 70%-80% confluency. The medium was replaced with DMEM/HG containing 1μM AZA or 300nM TSA, and the cells were cultured for 72 h. The control cells were cultured in DMEM/HG containing 1μM DMSO.

Methylation-specific quantitative PCR (MSP)

The CpG islands in the miR-133a gene were predicted using the website http://cpgislands.usc.edu, and one CpG island was detected in its promoter region. Genomic DNA was extracted from the A172 and U251 cells using a DNA extraction kit as per the manufacturer's instructions, and the purity and concentration were determined using an ultraviolet spectrophotometer. The DNA was modified with bisulfite using the EpiTect Bisulfite kit according to the manufacturer's instructions, and the methylated and unmethylated miR-133a were amplified using the following primers: methylated - forward 5'-GGTTGTTTGTTTTTTGGTTCG-3' and reverse 5'-ATCCTAAAACTACCCAAAATCGTA-3'; unmethylated - forward 5'-GGGATGAGGATTAGGATTTT-3' and reverse 5'-CAAACAAAACACAATAAAAACAAACA-3'. The PCR cycling conditions were: pre-denaturation at 94°C (3 min), followed by 35 cycles of denaturation at 94°C (30s), demethylation at 53°C (30s) and extension at 72°C (90s), and final extension at 94°C for 5 min. Generation of an amplified product with either methylated or unmethylated primers respectively indicated presence and absence of methylated sequences in the genome. Generation of amplified products with both primer pairs implied partial methylation. The methylation level of miR-133a gene was calculated by the ΔΔCt method. The experiment was repeated thrice.

Statistical analysis

Statistical analysis was performed using SPSS 19.0, R-2.15.3 and GraphPad Prism 5.0. The data were expressed as (X±S). One-way ANOVA was used for inter-group comparison, and independent-sample t test for comparing two groups. Kaplan-Meier method was used to draw survival curve and perform Log-rank tesk. *P* values< 0.05 were considered statistically significant.

Abbreviations

miRNAs: MicroRNAs; PPARγ: Peroxisome proliferator-activated receptor γ; CdK4: cycling-dependent killdeer 4; MSP: Methylation-specific quantitative PCR; UTR: 3' untranslated region

Declarations

Ethics approval and consent to participate

This study was approved by the Ethics Committee of Second Affiliated Hospital of Shenzhen University (SSZU20180307). All samples and data were collected after obtaining the statement on informed consent from the glioma patients or the legally authorized representatives of healthy controls with brain trauma.

Consent for publication

Not applicable.

Availability of data and material

Not applicable.

Competing interests

The author declares that he/she has no competing interests.

Funding

Not applicable.

Authors' contributions

YZ conceived the overall study idea approved the manuscript. LL conceptualized the study plan, performed the experiments and wrote the original manuscript. ZZ and XL analyzed the data. All authors have read and approved the manuscript.

Acknowledgements

The study was supported by the Second Affiliated Hospital of Shenzhen University in Shenzhen, China.

References

1. Ostrom QT, Gittleman H, Liao P, Vecchione-Koval T, Wolinsky Y, Kruchko C and Barnholtz-Sloan JS. CBTRUS statistical report: primary brain and other central nervous system tumors diagnosed in the United States in 2010–2014. Neuro-oncology. 2017;19:1-88. https://doi.org/10.1093/neuonc/nox158
2. Nam JY and De JG. Treatment of Glioblastoma. Journal of Oncology Practice. 2017;13:629-638. https://doi.org/10.1200/JOP.2017.025536
3. Zhou Q, Liu J, Quan J, Liu W, Tan H and Li W. microRNAs as potential biomarkers for the diagnosis of glioma: A systematic review and meta-analysis. Cancer Science. 2018;109:2651-2659. https://doi.org/10.1111/cas.13714
4. Stefano C, Suzanne E, Monica R, Daniela W, Johan H, Catharina L and Weng-Onn L. MicroRNA expression profiles associated with mutational status and survival in malignant melanoma. Journal of Investigative Dermatology. 2010;130:2062-2070. https://doi.org/10.1038/jid.2010.63
5. Fuyou Z, Jie L, Huaiyong G, Yumei L, Ri W, Haoran Z, Qiong W and Yuqing C. MiRNA profile of osteosarcoma with CD117 and stro-1 expression: miR-1247 functions as an onco-miRNA by targeting MAP3K9. International Journal of Clinical & Experimental Pathology. 2015;8:1451-1458. https://doi.org/PMC4396303
6. Seo YE, Suh HW, Bahal R, Josowitz A, Zhang J, Song E, Cui J, Noorbakhsh S, Jackson C and Bu T. Nanoparticle-mediated intratumoral inhibition of miR-21 for improved survival in glioblastoma. Biomaterials. 2019;201:87-98. https://doi.org/10.1016/j.biomaterials.2019.02.016
7. Huo L, Wang B, Zheng M, Zhang Y, Xu J, Yang G and Guan Q. miR1283p inhibits glioma cell proliferation and differentiation by targeting NPTX1 through IRS1/PI3K/AKT signaling pathway. Experimental and therapeutic medicine. 2019;17:2921-2930. https://doi.org/10.3892/etm.2019.7284
8. Liu F, Sang M, Meng L, Gu L, Liu S, Li J and Geng C. miR-92b promotes autophagy and suppresses viability and invasion in breast cancer by targeting EZH2. International Journal of Oncology. 2018;53:1505-1515. https://doi.org/10.3892/ijo.2018.4486
9. Shi L, Fei X, Wang Z and You Y. PI3K inhibitor combined with miR-125b inhibitor sensitize TMZ-induced anti-glioma stem cancer effects through inactivation of Wnt/β-catenin signaling pathway. In Vitro Cellular & Developmental Biology - Animal. 2015;51:1047-1055. https://doi.org/10.1007/s11626-015-9931-x
10. Currently. MicroRNA-31 Function as a Suppressor Was Regulated by Epigenetic Mechanisms in Gastric Cancer. BioMed Research International. 2017;2017:1-11. https://doi.org/10.1155/2017/5348490
11. Zare M, Bastami M, Solali S and Alivand MR. Aberrant miRNA promoter methylation and EMT-involving miRNAs in breast cancer metastasis: Diagnosis and therapeutic implications. Journal of Cellular Physiology. 2017;233:3729-3744. https://doi.org/10.1002/jcp.26116
12. Ramassone A, Pagotto S, Veronese A and Visone R. Epigenetics and MicroRNAs in Cancer. International Journal of Molecular Sciences. 2018;19:459-487.

https://doi.org/10.3390/ijms19020459

13. Cai W, Yang T, Liu H, Han L, Zhang K, Hu X, Zhang X, Yin KJ, Gao Y and Bennett M. Peroxisome proliferator-activated receptor γ (PPARγ): A master gatekeeper in CNS injury and repair. Progress in Neurobiology. 2018;163-164:27-58. https://doi.org/10.1016/j.pneurobio.2017.10.002
14. Chang WH and Lai AG. The pan-cancer mutational landscape of the PPAR pathway reveals universal patterns of dysregulated metabolism and interactions with tumor immunity and hypoxia. Annals of the New York Academy of Sciences. 2019;1448:65-82. https://doi.org/10.1111/nyas.14170
15. Wei-Hao S, Guo-Sheng C, Xi-Long O, Ye Y, Cheng L, Yuan Z, Yun S, Hai-Chen X, Bin X and Yi-Ping X. Inhibition of COX-2 and activation of peroxisome proliferator-activated receptor gamma synergistically inhibits proliferation and induces apoptosis of human pancreatic carcinoma cells. Cancer Letters. 2009;275:247-255. https://doi.org/10.1016/j.canlet.2008.10.023
16. Shu-Lan Y, Chiao-Lin Y, Shu-Ting C and Cheng-Hung C. Plasma rich in quercetin metabolites induces G2/M arrest by upregulating PPAR-γ expression in human A549 lung cancer cells. Planta Medica. 2011;77:992-998. https://doi.org/10.1055/s-0030-1250735
17. Xu F, Li F, Zhang W, Jia P. Growth of glioblastoma is inhibited by miR-133-mediated EGFR suppression. Tumour Biol 2015;36:9553. https://doi.org/10.1007/s13277-015-3724-4
18. Shen Y, Chen F, Liang Y. MicroRNA-133a inhibits the proliferation of non-small cell lung cancer by targeting YES1. Oncol Lett 2019;18:6759. https://doi.org/10.1016/j.cellsig.2014.08.012
19. Wang J, Yang ZY, Guo YF, Kuang JY, Bian XW and Yu SC. Targeting different domains of gap junction protein to control malignant glioma. Neuro Oncol. 2017;20:885-896. https://doi.org/10.1093/neuonc/nox207
20. Liu Z, Zhang Z, Yao J, Xie Y, Dai Q, Zhang Y and Zhou L. Serum extracellular vesicles promote proliferation of H9C2 cardiomyocytes by increasing miR-17-3p. Biochem Biophys Res Commun. 2018;499:441-446. https://doi.org/10.1016/j.bbrc.2018.03.157
21. Lu L, Miu KK, Shen G, Cheung HH and Chan WY. Comparison of multi-lineage differentiation of hiPSCs reveals novel miRNAs that regulate lineage specification. Scientific Reports. 2018;8:9630-9645. https://doi.org/10.1038/s41598-018-27719-0
22. Ma J, Fan Y, Zhang J, Feng S, Hu Z, Qiu W, Long K, Jin L, Tang Q and Wang X. Testosterone-Dependent miR-26a-5p and let-7g-5p Act as Signaling Mediators to Regulate Sperm Apoptosis via Targeting PTEN and PMAIP1. International Journal of Molecular Sciences. 2018;19:1233-1251. https://doi.org/10.3390/ijms19041233
23. Mullany LE, Herrick JS, Sakoda LC, Samowitz W, John, Stevens, Wolff RK and Slattery ML. miRNA involvement in cell cycle regulation in colorectal cancer cases. Genes & Cancer. 2018;9:53-65. https://doi.org/10.18632/genesandcancer.167
24. Qiu H, Zhong J, Luo L, Tang Z, Liu N, Kang K, Li L and Gou D. Regulatory Axis of miR-195/497 and HMGA1-Id3 Governs Muscle Cell Proliferation and Differentiation. International Journal of Biological Sciences. 2017;13:157-166. https://doi.org/10.7150/ijbs.17440

25. Kawakami K, Enokidaa H, Tatarano S, Yoshino H, Kagara I, Gotanda T, Tachiwada T, Nishiyama K, Nohata N and Seki N. The functional significance of miR-1 and miR-133a in renal cell carcinoma. European Journal of Cancer. 2012;48:827-836. https://doi.org/10.1016/j.ejca.2011.06.030
26. Zhenguo C, Funan L, Guanqiao W, Yanshu L, Hongyan Z and Feng L. miR-133 is a key negative regulator of CDC42-PAK pathway in gastric cancer. Cellular Signalling. 2014;26:2667-2673. https://doi.org/10.1016/j.cellsig.2014.08.012
27. Jung M, Brüne B, Knethen AV, Guiteras R, Cruzado JM, Hotter G and Sola A. Lipocalin-2 abrogates epithelial cell cycle arrest by PPARγ inhibition. Laboratory Investigation. 2018;98:1-15. https://doi.org/10.1038/s41374-018-0098-4
28. Chen K, Guo Z, Luo Y, Yuan J and Mo Z. UHRF1 Promotes Proliferation of Human Adipose-Derived Stem Cells and Suppresses Adipogenesis via Inhibiting Peroxisome Proliferator-Activated Receptor γ. BioMed research international. 2019;2019:1-9. https://doi.org/10.1155/2019/9456847
29. Jung M, Brüne B, Knethen AV, Guiteras R, Cruzado JM, Hotter G and Sola A. Lipocalin-2 abrogates epithelial cell cycle arrest by PPARγ inhibition. Laboratory Investigation. 2018;98:1408-1422. https://doi.org/10.1038/s41374-018-0098-4
30. Örd M, Venta R, Möll K, Valk E and Loog M. Cyclin-Specific Docking Mechanisms Reveal the Complexity of M-CDK Function in the Cell Cycle. Molecular cell. 2019:76-89. https://doi.org/10.1016/j.molcel.2019.04.026
31. Ren J, Singh BN, Qiang H, Li Z, Gao Y, Mishra P, Yi LH, Li J, Dowdy SC and Jiang SW. DNA hypermethylation as a chemotherapy target. Cellular Signalling. 2011;23:1082-1093. https://doi.org/10.1016/j.cellsig.2011.02.003
32. Lea AJ, Vockley CM, Johnston RA, Del Carpio CA, Barreiro LB, Reddy TE and Tung J. Genome-wide quantification of the effects of DNA methylation on human gene regulation. ELife. 2018;7:37513-37527. https://doi.org/10.1101/146829
33. Louis DN, Perry A, Reifenberger G, Deimling AV, Figarella-Branger D, Cavenee WK, Ohgaki H, Wiestler OD, Kleihues P and Ellison DW. The 2016 World Health Organization Classification of Tumors of the Central Nervous System: a summary. Acta Neuropathologica. 2016;131:803-820. https://doi.org/10.1007/s00401-016-1545-1
34. Yuan Y, Zhang H, Liu X, Lu Z, Li G, Lu M, Tao X. MicroRNA signatures predict prognosis of patients with glioblastoma multiforme through the Cancer Genome Atlas. Oncotarget 2017;8:58386. https://doi.org/10.18632/oncotarget.16878

Figures

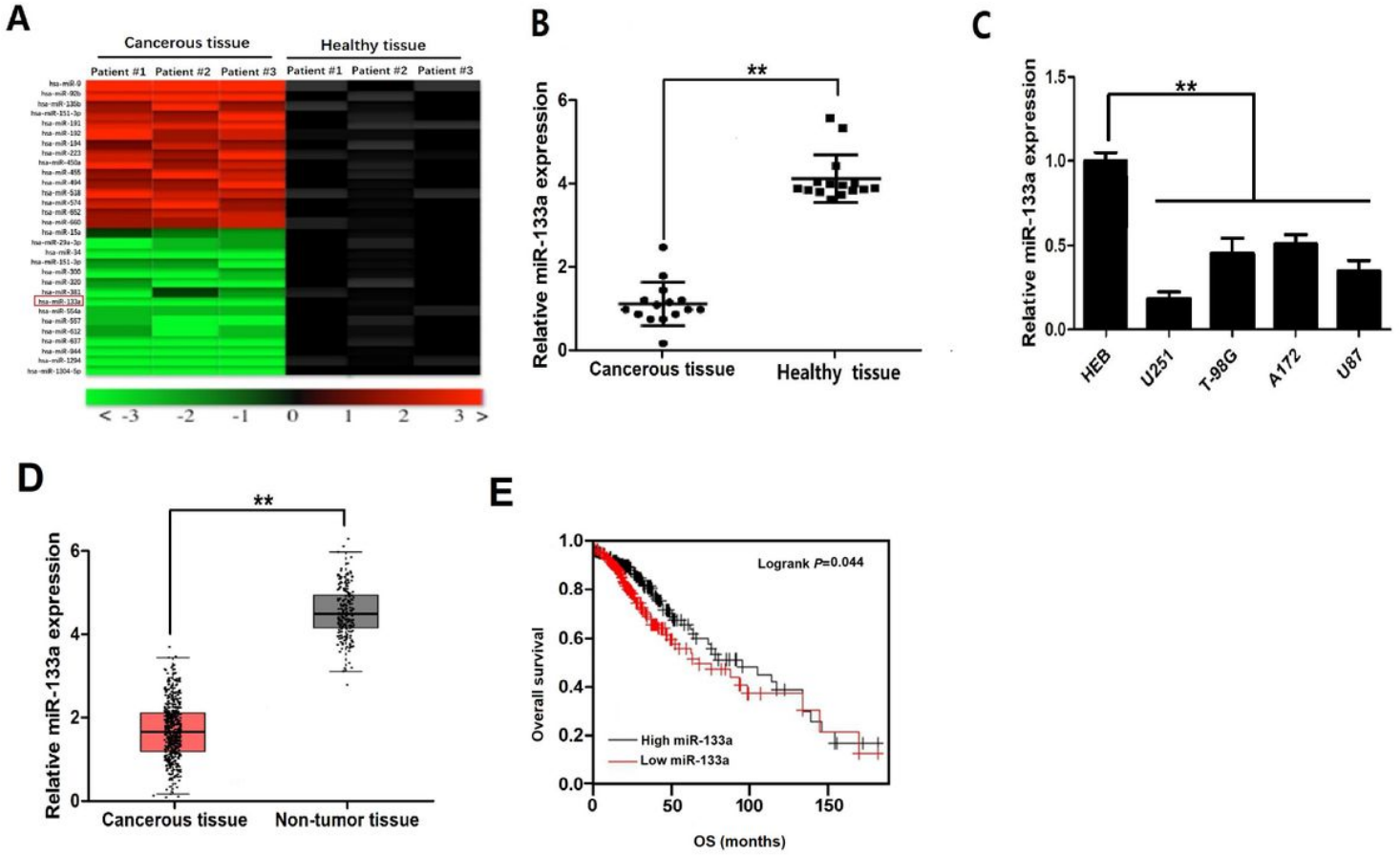

Figure 1

MiR-133a levels are aberrantly low in glioma and related with survival of glioma patients. A. Heat map of 30 differentially expressed miRNAs ($p<0.01$) in the microarray analysis (red indicates up-regulation and green indicates down-regulation). B. RT-PCR results showing miR-133a levels in 15 glioma and normal brain tissue samples. C. RT-PCR results showing miR-133a levels in various cell lines; D: The incidence of low levels of miR-133a in glioma patients was evaluated using TCGA dataset; E: Overall survival (OS) curves of Kaplan-Meier analysis; * * $p<0.01$.

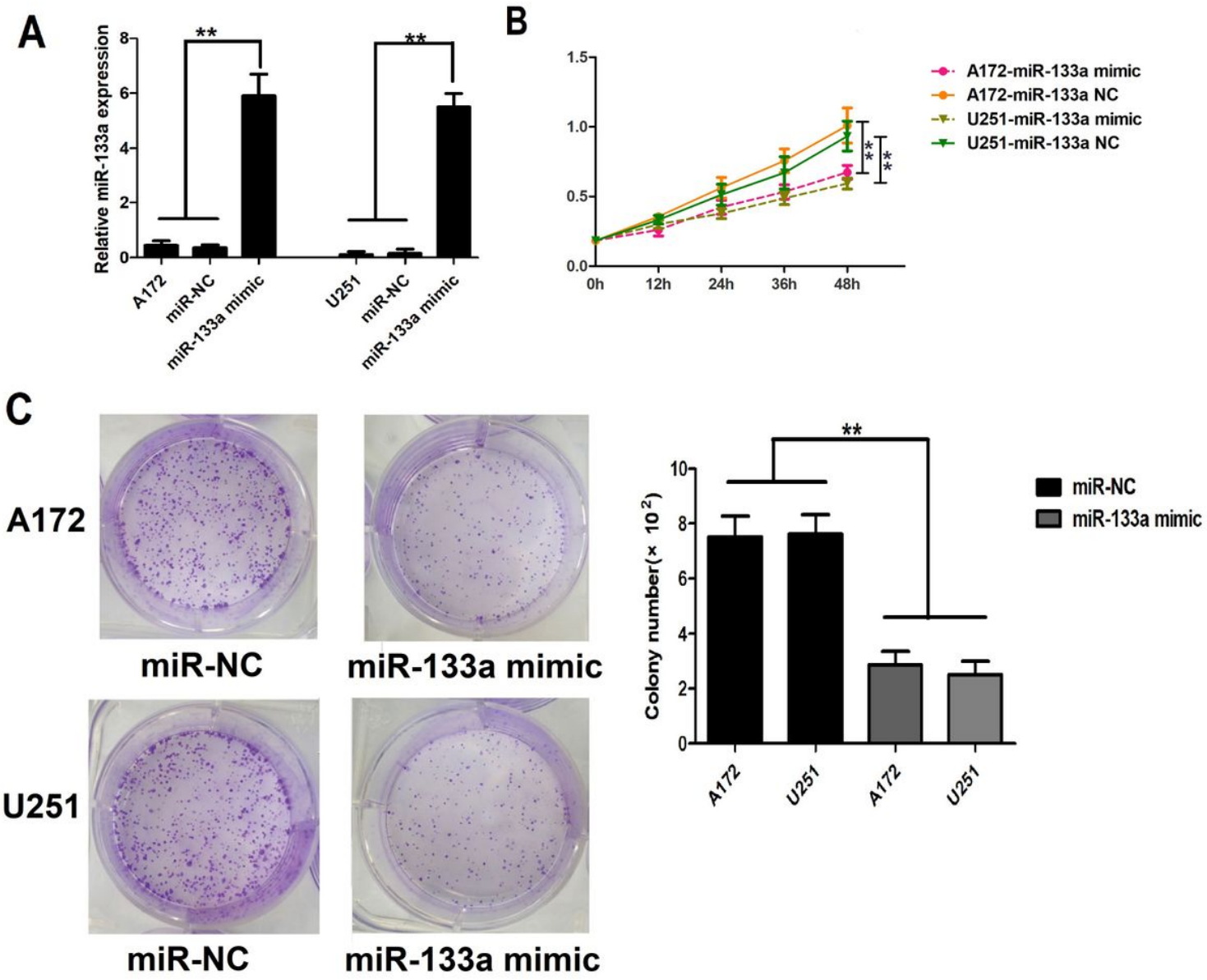

Figure 2

Overexpression of miR-133a inhibits the proliferation of glioma cells: A. Expression levels of miR-133a in the A172 and U251 cells transfected with the miR-133a mimic. B. Proliferation rate of control and miR-133a-overexpressing glioma cells. C. Number of colonies formed by glioma cells transfected with miR-133a mimic or miR-NC. **p<0.01

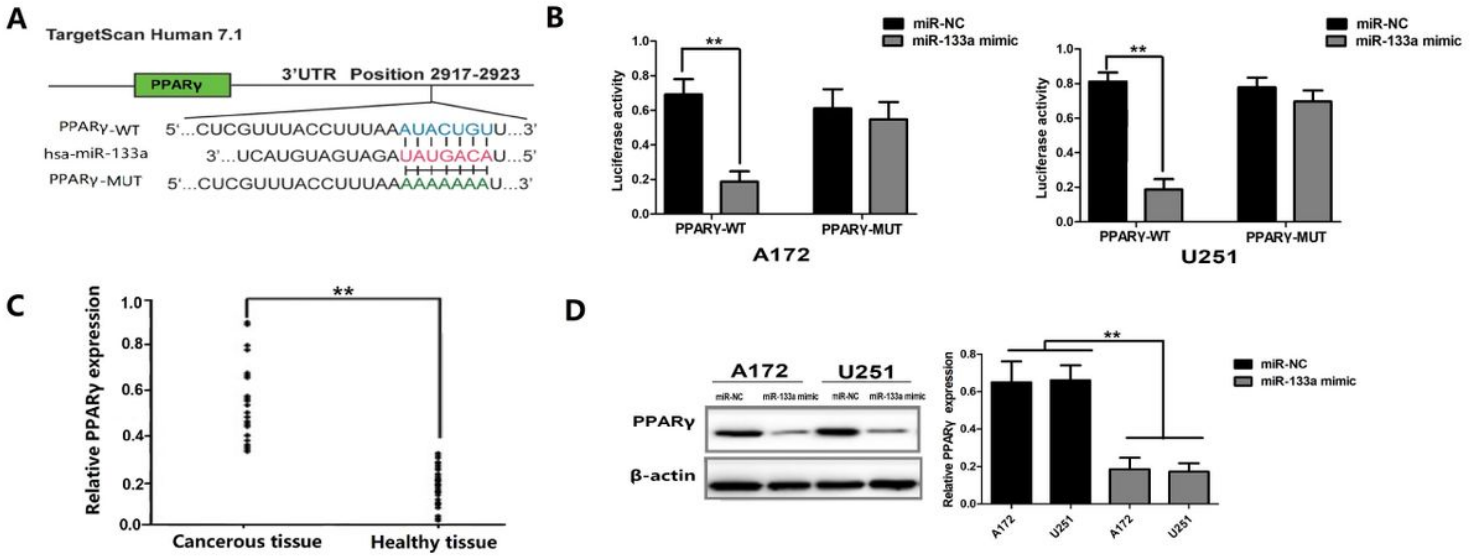

Figure 3

MiR-133a inhibits PPARγ expression in glioma cells. TargetScan prediction results. B. Dual luciferase gene reporter assay result. C. Immunoblots showing PPARγ levels in glioma and normal tissue samples. D. Immunoblots showing PPARγ levels in A172 and U251 cells transfected with miR-133a mimic or miR-NC. **p<0.01

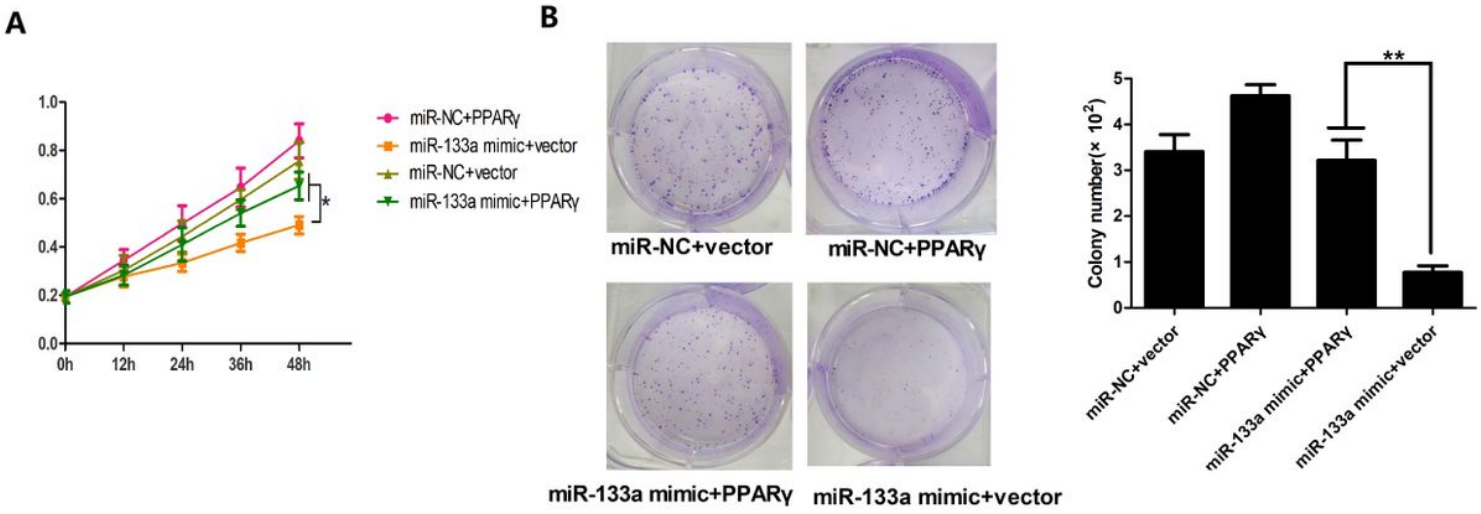

Figure 4

MiR-133a inhibits the proliferation of glioma cells by down-regulating PPARγ. A. MiR-133a inhibits the proliferation of glioma cells by down-regulating PPARγ. B. MiR-133a suppresses the colony forming ability of glioma cells by down-regulating PPARγ; *p<0.05, **p< 0.01

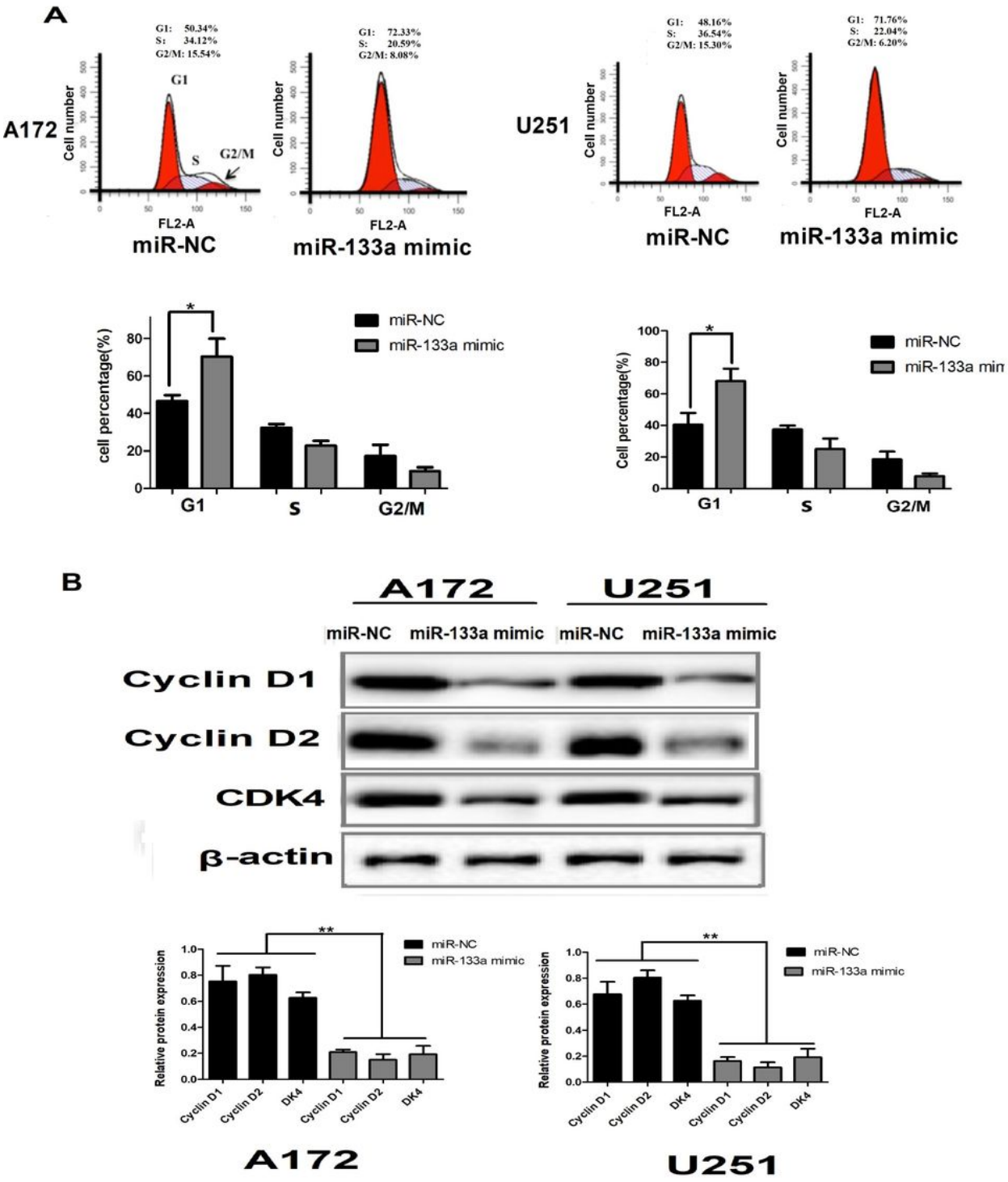

Figure 5

MiR-133a inhibits the progression of glioma cell cycle. A. Flow cytometry plots showing the cell cycle distribution of miR-133a-overexpressing and control glioma cells. B. Immunoblots showing the expression levels of CyclinD1, Cyclin D2 and CDK4 in glioma cells following miR-133a overexpression.

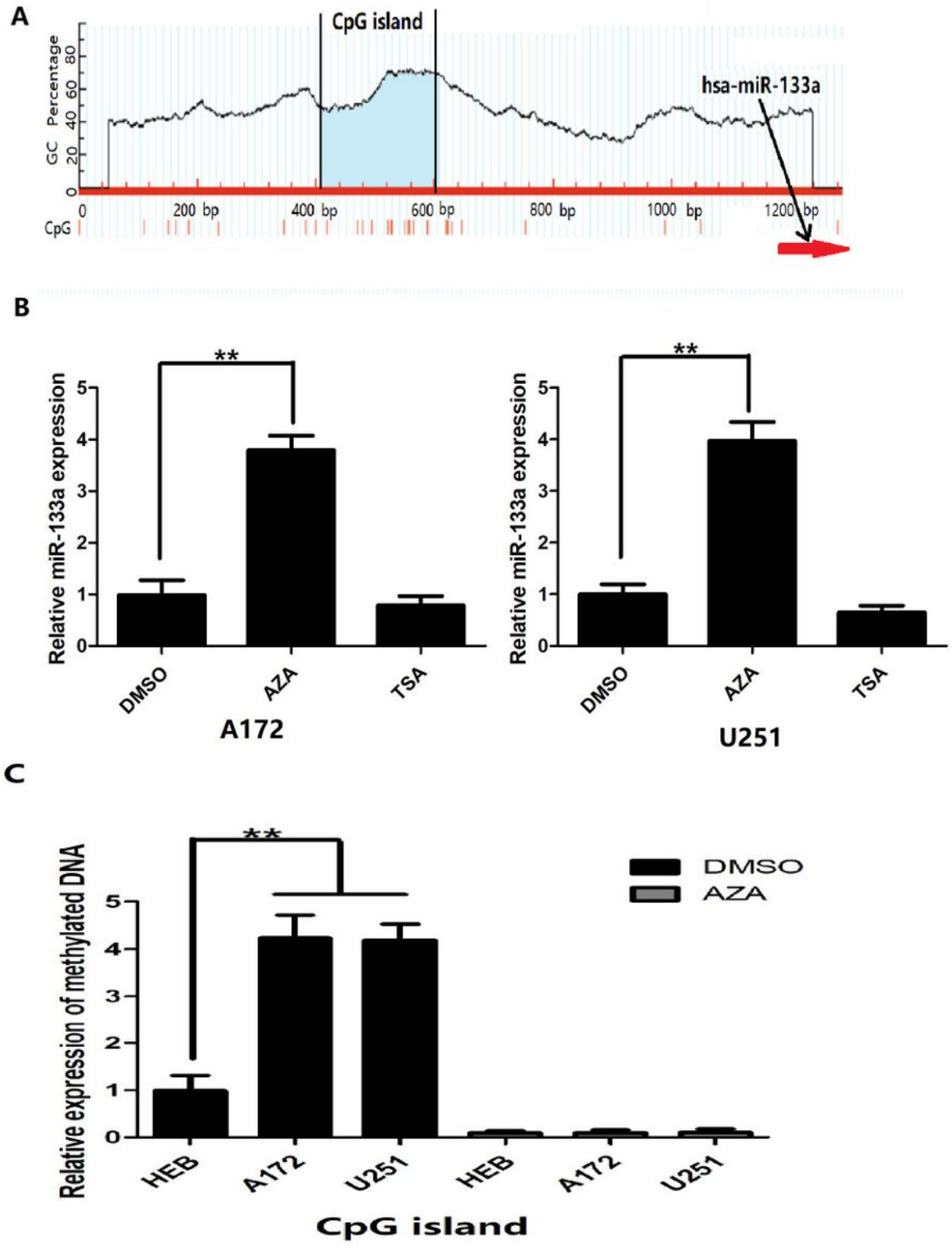

Figure 6

DNA methylation inhibits the expression of miR-133a in glioma cells. A. CpG island location in miR-133a gene promoter region. B. MiR-133a expression levels in control and AZA-treated glioma cells. C. Extent of DNA methylation in miR-133a promoter region in the normal glial cell line HEB and glioma cell lines A172 and U251.

Supplementary Files

This is a list of supplementary files associated with this preprint. Click to download.

- SupplementaryMaterials.docx